Electrical conductivity of dense metal plasmas

Ronald Redmer
Universität Rostock, Fachbereich Physik, Universitätsplatz 3, D-18051 Rostock, Germany
(Received 8 September 1998)

The composition of dense metal plasmas is calculated considering higher ionization stages of the atoms. A system of coupled mass action laws is solved self-consistently taking into account medium corrections which lead to pressure ionization at high densities. The electrical conductivity is calculated within linear response theory. The interactions between the various species are treated on *T* matrix level. The numerical results for the electrical conductivity are in reasonable agreement with new experimental data for nonideal Al and Cu plasmas. Comparison with other theories is performed.
[S1063-651X(99)04101-X]

PACS number(s): 52.25.Fi, 52.25.Jm, 05.60.Cd, 51.10.+y

I. INTRODUCTION

The electrical conductivity of strongly coupled plasmas is a fundamental quantity for the characterization of the plasma state. For instance, the transport coefficients of fully ionized hydrogen (and helium) plasma are relevant for the description of the physical properties of the interiors of the giant planets or white dwarfs [1–3]. In the famous shock wave experiments of Ivanov *et al.* [4] the conductivity of rare gas plasmas has been determined for coupling parameters $\Gamma \leqslant 2$. New techniques such as capillary discharges [5] or ultrashort high-intensity laser pulses on solid targets [6] have been developed over the last ten years so that the strongly coupled plasma domain with $\Gamma \gg 1$ is now accessible.

Especially, the technique of rapid wire evaporation was applied successfully to generate expanded fluid metals and metal plasmas with coupling parameters up to $\Gamma \approx 200$ [7–12]. The electrical conductivity was determined for various metals such as copper, aluminum, tungsten, zinc, and molybdenum for the density and temperature range from near solid density and room temperature to 0.001 solid density and some 10 eV temperature, depending on the details of the experimental setup. Experiments for carbon plasma are in progress [13].

Interesting features have been observed in these experiments. First, the conductivity shows a minimum around $0.1 \mathrm{g/cm}^3$ in the expanded metal vapor. This behavior of the plasma conductivity has been predicted theoretically a long time ago; for a review, see [14]. Second, the conductivity becomes a universal function of the coupling parameter Γ for high densities.

Theoretical studies of the transport properties of strongly coupled plasmas are mainly based on standard kinetic theory [15] or the Ziman theory for fluid metals [16,17]. We will use here linear response theory in the formulation of Zubarev [18–20] to calculate the electrical conductivity of metal plasmas within a partially ionized plasma model. This approach has already been applied to determine the transport coefficients of hydrogen plasma [21] and fluid alkali metals [22] in a large domain of the density-temperature domain. We compare our results with available experimental data for metal plasmas and the standard theories mentioned above. The results of a self-consistent field theory of Tkachenko and Fernández de Córdoba [23] which is based on a generalized random phase approximation for strongly coupled, fully ionized, multicomponent plasmas are given in addition.

II. PLASMA COMPOSITION

A. Mass action laws

In this paper, we treat dense metal plasmas consisting of electrons and various ion species such as M^{1+}, M^{2+}, M^{3+}, etc. We will apply the approach to aluminum and copper plasmas, i.e., $M = \mathrm{Al}$, Cu. Neutrality requires that $n_e = n_{1+} + 2n_{2+} + 3n_{3+} + \cdots$, where n_{k+} is the partial density of the k-fold ionized species M^{k+} and n_e the electron density. The total ion density is given by $n_i = n_{1+} + n_{2+} + n_{3+} + \cdots$. Besides the charged components, also neutral atoms M^0 and dimers M_2^0 may occur especially for low temperatures, so that the partially ionized plasma (PIP) model applies.

The composition of such a multicomponent plasma is determined by the possible reactions between the various species. We consider here the following ionization processes:

$$M^0 \rightleftharpoons M^{1+} + e,$$
$$M^{1+} \rightleftharpoons M^{2+} + e, \tag{1}$$
$$M^{2+} \rightleftharpoons M^{3+} + e.$$

Higher charged and neutral clusters are negligible. The respective partial densities are derived from the coupled chemical equilibria for given parameters such as temperature and total mass density,

$$\mu_0 + E_{\mathrm{ion}}^{(1)} = \mu_{1+} + \mu_e,$$
$$\mu_{1+} + E_{\mathrm{ion}}^{(2)} = \mu_{2+} + \mu_e, \tag{2}$$
$$\mu_{2+} + E_{\mathrm{ion}}^{(3)} = \mu_{3+} + \mu_e.$$

The energies necessary for the excitation of the different ionization states $(k+)$ are denoted by $E_{\mathrm{ion}}^{(k)}$ and are given for Al and Cu in Table I up to $k = 3$.

The chemical potentials are usually split into an ideal and an interaction part according to

TABLE I. Parameters for the evaluation of the coupled mass action laws according to Eq. (7) and the molar masses M_{mol} for Al and Cu.

	Al	Cu
Z	13	29
$E_{\mathrm{ion}}^{(1)}$ in eV	5.986	7.726
$E_{\mathrm{ion}}^{(2)}$ in eV	18.829	20.293
$E_{\mathrm{ion}}^{(3)}$ in eV	28.448	36.841
α_D in a_B^3	56.28	41.165
r_0 in a_B	1.86	1.61
M_{mol} in g/mol	26.982	63.546

$$\mu_\alpha = \mu_\alpha^{\mathrm{id}} + \mu_\alpha^{\mathrm{int}}, \tag{3}$$

where $\{\alpha\}=\{e,1+,2+,3+,0\}$. The relation between the ideal part of the chemical potentials and the respective number densities is given for arbitrary degeneracy by Fermi integrals $F_{1/2}(x)$ of the order 1/2. Defining dimensionless quantities according to

$$x_\alpha = \beta\mu_\alpha^{\mathrm{id}},\ y_\alpha = n_\alpha \Lambda_\alpha^3 / g_\alpha, \tag{4}$$

where $\beta = 1/(k_B T)$ is the inverse temperature, $\Lambda_\alpha^2 = 2\pi\beta\hbar^2/m_\alpha$ is the thermal wavelength of species α, and g_α is the sum over the internal degrees of freedom (spin), we have

$$y_\alpha = F_{1/2}(x_\alpha). \tag{5}$$

Considering the densities as independent variables, the inverse function

$$x_\alpha = U_{1/2}(y_\alpha) \tag{6}$$

is of more practical interest. Efficient Padé approximations for this relation can be found in Ref. [24].

The heavy particle ions and atoms can be described classically and Eq. (6) reads for this case $x_\alpha = \ln(y_\alpha)$. The spin factors for Al and Cu are $g_0=2$, $g_1=1$, $g_2=2$, and $g_3=2$. Combining Eqs. (2)–(6), the following mass action laws can be derived for the composition of a dense metal plasma with higher ionization stages up to $k=3$:

$$\begin{aligned} n_0 &= 2 n_{1+} \exp[\beta(\mu_e^{\mathrm{id}} + E_{\mathrm{ion}}^{(1)} + \Delta\mu_1)], \\ n_{1+} &= \tfrac{1}{2}\, n_{2+} \exp[\beta(\mu_e^{\mathrm{id}} + E_{\mathrm{ion}}^{(2)} + \Delta\mu_2)], \\ n_{2+} &= 2 n_{3+} \exp[\beta(\mu_e^{\mathrm{id}} + E_{\mathrm{ion}}^{(3)} + \Delta\mu_3)]. \end{aligned} \tag{7}$$

The quantities $\Delta\mu_k = \mu_e^{\mathrm{int}} + \mu_k^{\mathrm{int}} - \mu_{k-1}^{\mathrm{int}}$ are given by the interaction contributions to the chemical potentials and yield a shift of the chemical equilibria compared with the ideal Saha equations. They can be interpreted as lowering of the respective ionization energies $E_{\mathrm{ion}}^{(k)}$ with increasing density which leads to pressure ionization or the Mott effect. The consistent calculation of these shifts is the central problem for the determination of the plasma composition.

B. Medium corrections

The interaction contributions to the chemical potential $\mu_\alpha^{\mathrm{int}}$ can be derived from the respective one-particle self-energy using standard methods of many-particle theory such as the Green function technique (for details, see [21,25]). Considering the lowest orders of a perturbative expansion with respect to the screened Coulomb potential, the Hartree-Fock and Montroll-Ward contributions are relevant. A polarization contribution occurs in addition due to the possible interactions of the charged particles with neutral atoms.

In order to characterize the plasma state, we introduce the Coulomb coupling constant Γ for the ion system with an effective ionization state Z_{eff} and the degeneracy parameter Θ for the electron system [26],

$$\Gamma = \frac{(Z_{\mathrm{eff}} e)^2}{4\pi\varepsilon_0 k_B T d},\ \Theta = \frac{k_B T}{E_F}. \tag{8}$$

E_F denotes the Fermi energy of electrons and d is the mean distance between the heavy particles (ions),

$$E_F = \frac{\hbar^2}{2m_e}(3\pi^2 n_e)^{2/3},\ d = \left(\frac{3}{4\pi n_i}\right)^{1/3}. \tag{9}$$

Efficient interpolation formulas have been constructed by Ebeling and Richert [27,28] for the interaction contributions to the chemical potential μ^{int} and the free energy density f^{int} of a fully ionized, two-component electron-ion plasma. These Padé approximations interpolate between the known limiting cases for the behavior of the thermodynamic quantities of a fully ionized plasma: the nondegenerate case $\Theta \gg 1$ (Debye-Hückel theory), the strong coupling limit for the electrons $r_s = d/a_B \ll 1$ (Gell-Mann–Brueckner result; $a_B = 0.529\,177\,2 \times 10^{-10}$ m is the Bohr radius), and the case of strongly correlated ions $\Gamma \gg 1$ (Madelung energy). These formulas cover the whole density region from the dilute plasma to the dense fluid state within an estimated maximum error of about 20%.

The expressions for the free energy density have been generalized by Förster [29] for the case of a fully ionized, multicomponent plasma with various ionization states. The correlations in the Coulomb system can be split into an electron, ion, and electron-ion term,

$$\begin{aligned} f^{\mathrm{int}}(n_e, n_i, T) &= f_e^{\mathrm{gas}}(n_e, T) + f_i^{\mathrm{gas}}(n_i, T) \\ &\quad + f_{ie}^{\mathrm{int}}(n_e, n_i, T). \end{aligned} \tag{10}$$

The rather lengthy analytical expressions can be found in the literature [30]. The interaction contributions to the chemical potentials needed for the evaluation of the mass action laws (7) are derived numerically from Eq. (10) via

$$\mu_\alpha^{\mathrm{int}} = \left(\frac{\partial f^{\mathrm{int}}}{\partial n_\alpha}\right)_T. \tag{11}$$

For partial ionization, a polarization contribution arises due to the interaction between charged particles and neutral atoms which has been calculated for arbitrary densities for the interaction of electrons with hydrogen and alkali metal atoms [31]. The results can be given in a parametrized form

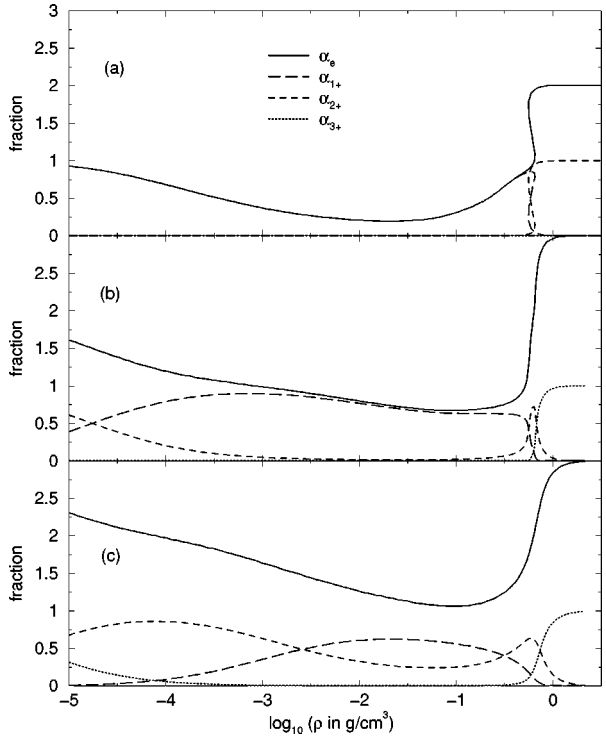

FIG. 1. Composition of Al plasma as a function of the mass density ϱ for various temperatures: (a) 10^4 K, (b) 2×10^4 K, (c) 3×10^4 K. Electrons: solid line, Al^{1+}: long-dashed line, Al^{2+}: dashed line, Al^{3+}: dotted line (negligible for $T\leqslant10^4$ K).

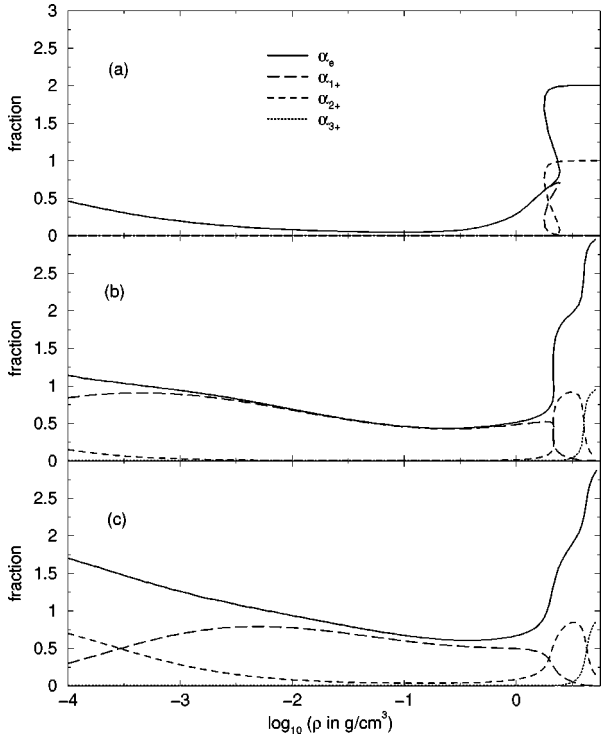

FIG. 2. Composition of Cu plasma as a function of the mass density ϱ for various temperatures: (a) 10^4 K, (b) 2×10^4 K, (c) 3×10^4 K. Electrons: solid line, Cu^{1+}: long-dashed line, Cu^{2+}: dashed line, Cu^{3+}: dotted line (negligible for $T\leqslant10^4$ K).

as linearized virial coefficients $B^{\rm PP}$ with respect to a screened, local polarization potential $V^{\rm PP}(R)$ [32],

$$\mu_{eM^0}^{\rm int}=n_0B^{\rm PP},\ B^{\rm PP}=\int d^3R\,V^{\rm PP}(R),$$
$$V^{\rm PP}(R)=-\frac{e^2\alpha_D\exp(-2\kappa R)}{2(4\pi\varepsilon_0)^2(R^2+r_0^2)^2}(1+\kappa R)^2. \tag{12}$$

The cutoff radius r_0 is estimated from the relation [33]

$$r_0^4=\alpha_D a_B/2Z^{1/3}. \tag{13}$$

The dipole polarizability α_D, the nuclear charge number Z, and the cutoff radius r_0 are summarized for Al and Cu in Table I. The inverse screening length $\kappa=1/R_D$ is given for arbitrary degeneracy by Fermi integrals $F_{-1/2}(x)$ of the order $-1/2$ [24],

$$\kappa^2=\frac{\beta e^2}{\varepsilon_0}\frac{2}{\Lambda_e^3}F_{-1/2}(\beta\mu_e^{\rm id}). \tag{14}$$

Inserting the interaction contributions of the chemical potentials via Eqs. (10)–(12) into the mass action laws (7), the composition of the plasma can be characterized by the following quantities dependent on temperature and total mass density:

$$\alpha_e=n_e/(n_0+n_i),\ \alpha_{k+}=n_{k+}/(n_0+n_i). \tag{15}$$

The ionization degree α_e is the average number of free electrons generated per ion, while α_{k+} denote the relative fractions of the ion species M^{k+} with respect to the total number of heavy particles.

Besides the composition, the equation of state of the plasma is of interest which can be derived from the relation [25]

$$p(\varrho,T)=\sum_\alpha\,[n_\alpha\mu_\alpha(n_\gamma,T)-f_\alpha(n_\gamma,T)]. \tag{16}$$

The mass density ϱ is defined by the molar mass according to $\varrho=n_iM_{\rm mol}/L$ where $L=6.022\,137\times10^{23}\,{\rm mol}^{-1}$ is Avogadro's constant.

C. Results for the composition

In Figs. 1 and 2 we show the results for the composition of aluminum and copper plasma for various temperatures as a function of the mass density ϱ. The relative fraction of electrons and ions is defined via Eq. (15).

The behavior is very systematic. For low densities and high temperatures, the plasma is fully ionized. With increasing density and for lower temperatures, also the lower charged states M^{2+} and M^{1+} as well as neutral atoms M^0 occur in relevant fractions according to the mass action laws (7). The region where neutral atoms occur is characterized by $\alpha_e\leqslant1$. The higher charged states are again dominating for densities near or higher than the solid state density ϱ_0. For example, the twofold ionized states Al^{2+} and Cu^{2+} are the highest charged states for $T\leqslant10^4$ K so that there $\alpha_e=2$ and $\alpha_{2+}=1$. For higher temperatures, also the threefold ionized

states Al^{3+} and Cu^{3+} become operative so that there $\alpha_e = 3$ and $\alpha_{3+} = 1$ are the limiting values. The concentration of the higher charged states in copper plasmas is somewhat lower than in aluminum plasmas because of the higher ionization energies, see Table I.

The equation of state (16) shows an instability behavior at high densities around the solid state density ϱ_0 for $T \leqslant 15 \times 10^3$ K, i.e., $(\delta p/\delta V)_T \geqslant 0$, which has to be treated by a Maxwell construction. This instability manifests itself in an ambiguous behavior of the ionization degree as a function of the density, see Figs. 1 and 2.

This instability is connected with the theoretical plasma phase transition which has extensively been discussed for hydrogen and other elements, e.g., in [14,30]. Our aim is to compare the electrical conductivities with the available experimental data for the *expanded* solid (or fluid) domain. Therefore we will restrict ourselves in this paper to the density region with $\varrho \leqslant \varrho_0$. A detailed analysis of the instability region is necessary when treating shock compressed matter with $\varrho > \varrho_0$ which is not intended here. In that domain, the Thomas-Fermi theory and related equations of state such as the QEOS model [34] are applicable.

III. ELECTRICAL CONDUCTIVITY

A. Linear response method

The electrical conductivity σ and other transport coefficients such as the thermopower α and the thermal conductivity λ are well known for nondegenerate, low-density plasmas where the Spitzer theory [35] applies. For strongly coupled, degenerate systems such as fluid metals, the Ziman theory is applicable [36] and the electrical conductivity is given by the Ziman formula, the thermopower by the Mott formula, and the thermal conductivity by the Wiedemann-Franz relation.

Most of the theoretical attempts to describe the (electrical and thermal) conductivity of plasmas in a large density-temperature domain are based upon the Ziman formula which is, strictly speaking, only valid for the case of strongly coupled ions and degenerate electrons. Improvements account for many-particle effects such as, for instance, structure factor, local-field corrections, and arbitrary degeneracy [15–17,37]. On the other hand, improvements of the Spitzer theory have been proposed for the nondegenerate region of strongly coupled, partially ionized [38,39] as well as weakly nonideal [40–42] plasmas. Lee and More [43] evaluated the complete set of transport coefficients for electron transport in electric *and* magnetic fields within relaxation time approximation for a quantum transport (Boltzmann) equation for arbitrary degeneracy as well as partial ionization.

A general approach to the thermoelectric transport properties of Coulomb systems valid for arbitrary degeneracy has been derived within linear response theory, given here in an extended version originally developed by Zubarev [18] for mechanical and nonmechanical perturbations of an open system. Due to the relation between transport coefficients, correlation functions, and thermodynamic Green's functions [19,20], this efficient method allows for the treatment of many-particle effects and the consistent inclusion of the composition, as has been determined in the preceding section.

Postulating a linear response of the system with respect to the external electric field, the conductivity can be given in a determinant representation [44,45] which is known also from standard kinetic theory,

$$\sigma = \frac{e^2}{\Omega_0 |d|} \begin{vmatrix} 0 & \overline{N}_0 \\ N_0 & d \end{vmatrix}, \tag{17}$$

with the system volume Ω_0 and the abbreviations

$$\begin{gathered} \overline{N}_m = (\overline{N}_{m0} \quad \overline{N}_{m1} \quad \cdots \quad \overline{N}_{mL}), \\ N_m = \begin{pmatrix} N_{0m} \\ N_{1m} \\ \vdots \\ N_{Lm} \end{pmatrix}, \quad (d) = \begin{pmatrix} d_{00} & d_{01} & \cdots & d_{0L} \\ d_{10} & d_{11} & \cdots & d_{1L} \\ \vdots & \vdots & \ddots & \vdots \\ d_{L0} & d_{L1} & \cdots & d_{LL} \end{pmatrix}. \end{gathered} \tag{18}$$

The equilibrium correlation functions

$$\begin{gathered} \overline{N}_{nm} = N_{nm} + \frac{1}{m} \langle \mathbf{P}_n(\varepsilon); \dot{\mathbf{P}}_m \rangle, \\ N_{nm} = \frac{1}{m} (\mathbf{P}_n, \mathbf{P}_m), \\ d_{nm} = \langle \dot{\mathbf{P}}_n(\varepsilon); \dot{\mathbf{P}}_m \rangle, \\ \dot{\mathbf{P}}_n = \frac{i}{\hbar} [H_S, \mathbf{P}_n], \end{gathered} \tag{19}$$

are defined by

$$\begin{gathered} (A,B) = \int_0^\beta d\tau \, \mathrm{Tr}\{\rho_0 A(-i\hbar\tau) B\}, \\ \langle A(\varepsilon); B \rangle = \lim_{\varepsilon \to 0} \int_{-\infty}^0 dt \, e^{\varepsilon t} (A(t), B), \\ A(t) = e^{iH_S t/\hbar} A(0) e^{-iH_S t/\hbar}, \\ \varrho_0 = \frac{1}{Z_0} \exp\left(-\beta H_S + \beta \sum_\alpha \mu_\alpha N_\alpha \right). \end{gathered} \tag{20}$$

The system Hamiltonian H_S is given below, see Eq. (23). The generalized momenta $\mathbf{P}_n$ of the electron system,

$$\mathbf{P}_n = \sum_{\mathbf{k}} \hbar \mathbf{k} [\beta E_e(k)]^n a_e^\dagger(k) a_e(k), \tag{21}$$

are a set of relevant observables which characterize the nonequilibrium state. The terms of lowest order are related to the total electron momentum ($\mathbf{P}_0$) and the ideal part of the electron energy current ($\mathbf{P}_1$). They are connected with the microscopic expressions for the electrical current density and the electronic heat current density, respectively. A set of three momenta $\{n\} = \{0,1,2\}$, i.e., $L = 2$, is sufficient to determine the transport coefficients within 5% accuracy [45].

B. Evaluation of the correlation functions

Neglecting the terms $\langle \mathbf{P}_n(\varepsilon);\dot{\mathbf{P}}_m\rangle$ which are related to the Debye-Onsager relaxation effect, we have $\overline{N}_{nm}=N_{nm}$ in Eq. (19). The generalized particle numbers N_{nm} are given by Fermi integrals $F_n(x)$,

$$N_{nm}=N_e\frac{\Gamma(n+m+5/2)}{\Gamma(5/2)}\frac{F_{n+m+1/2}(\beta\mu_e^{\mathrm{id}})}{F_{1/2}(\beta\mu_e^{\mathrm{id}})}, \tag{22}$$

which were evaluated for given densities and temperatures.

The force-force correlation functions d_{nm} in Eq. (19) can be related to thermodynamic Green's functions. Applying a systematic diagram analysis, the Landau, Lenard-Balescu, and Boltzmann collision integrals can be derived (for details, see [14,21]). According to the system Hamiltonian,

$$H_S=\sum_{\mathbf{k}} E_e(k)a_e^{\dagger}(k)a_e(k) + \sum_{\alpha}\sum_{\mathbf{p,k,q}} V_{e\alpha}(q)\; a_e^{\dagger}(k+q)a_{\alpha}^{\dagger}(p-q)a_{\alpha}(p)a_e(k), \tag{23}$$

where $\alpha=\{e,1+,2+,3+\}$ denotes the species and $V_{e\alpha}(q)$ is the effective interaction between the charged particles, the correlation functions can be separated with respect to electron-electron, electron-ion, and electron-atom scattering, i.e.,

$$d_{nm}=D_{nm}^{ee}+D_{nm}^{ei}+D_{nm}^{ea}. \tag{24}$$

The correlation functions D_{nm} are evaluated on the level of the Boltzmann collision integral which corresponds to a T matrix approximation for the respective scattering process. They can be related to transport cross sections $Q_T^{e\alpha}$ given below as for the case of hydrogen [21]. The electron-electron term reads

$$D_{nm}^{ee}=\frac{4}{3}\sqrt{\frac{2m}{\pi\beta}}nN_e\int_0^{\infty}dx\,x^3R_{nm}(x)Q_T^{ee}(x)\exp(-x), \tag{25}$$

where $x=\beta\hbar^2k^2/m_e$. The polynomials R_{nm} can be found, e.g., in [14].

The total electron-ion contribution D_{nm}^{ei} represents the weighted sum of the scattering processes of electrons at all possible ion species via

$$D_{nm}^{ei}=\frac{2\hbar}{3\pi^2}N_i\int_0^{\infty}dk\,k^3[\beta E_e(k)]^{n+m}f_e(k)[1-f_e(k)] \times\left|\sum_{k+}\sqrt{\alpha_{k+}Q_T^{ek+}(k)}\right|^2. \tag{26}$$

The electron-atom contribution is given by

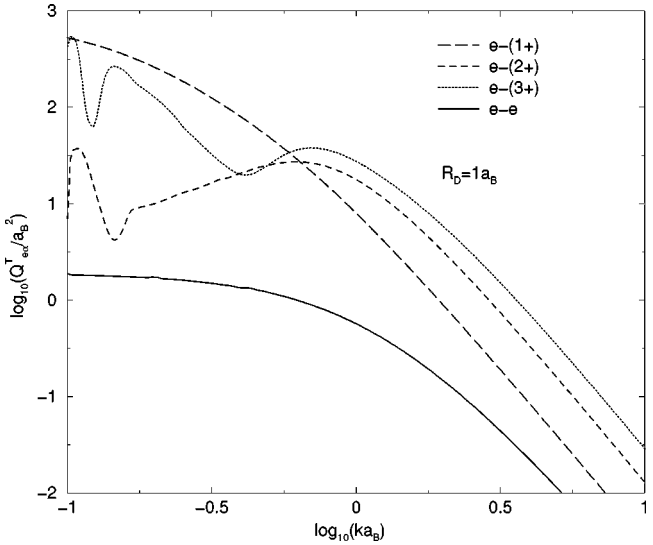

FIG. 3. Transport cross sections for electron scattering at single (long-dashed line), double (short-dashed line), and triple ionized atoms (dotted line) as well as for electron-electron scattering (full line). The interactions are modeled by the Debye potential (29) for a screening length of $R_D=1a_B$.

$$D_{nm}^{ea}=\frac{2\hbar}{3\pi^2}N_a\int_0^{\infty}dk\,k^3[\beta E_e(k)]^{n+m} \times f_e(k)[1-f_e(k)]\,Q_T^{ea}(k). \tag{27}$$

N_e, N_i, and N_a are the electron, total ion, and atom particle numbers.

The transport cross sections are determined by the scattering phase shifts δ_ℓ within a partial wave expansion with respect to the angular momentum ℓ according to $(d=e,a)$

$$Q_T^{ed}(k)=\frac{4\pi}{k^2}\sum_{\ell=0}^{\infty}(\ell+1)\sin^2[\delta_\ell^{ed}(k)-\delta_{\ell+1}^{ed}(k)],$$
$$Q_T^{ee}(k)=\frac{4\pi}{k^2}\sum_{\ell=0}^{\infty}\frac{(\ell+1)(\ell+2)}{2\ell+3}\left(1-\frac{(-1)^{\ell}}{2}\right) \times\sin^2[\delta_\ell^{ee}(k)-\delta_{\ell+2}^{ee}(k)]. \tag{28}$$

C. Results for the transport cross sections

The scattering phase shifts in Eqs. (28) are determined by solving the Schrödinger equation [46,47]. The simplest screened potential which models the interactions between the charged particles is the Debye potential

$$V_{e\alpha}^D(r)=\frac{Z_\alpha e^2}{4\pi\varepsilon_0 r}\exp(-\kappa r). \tag{29}$$

κ is the inverse Debye screening length according to Eq. (14) and $Z_\alpha=\{-1,+1,+2,+3\}$ is the charge of species α. The transport cross sections are shown in Figs. 3–5 as a function of the wave number k for $R_D=(1,10,100)\times a_B$.

For higher energies $k\geqslant 1a_B$, where the Born approximation becomes applicable, a systematic increase with Z_α occurs. For higher densities, i.e., lower screening lengths R_D,

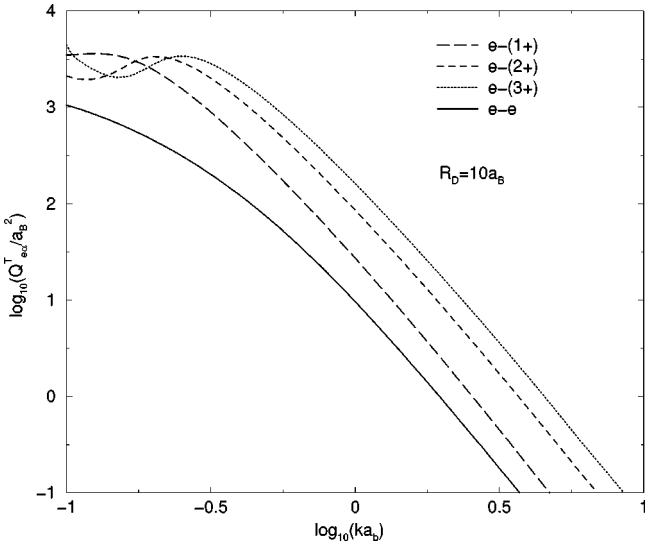

FIG. 4. Same as Fig. 3 but for a screening length of $R_D = 10a_B$.

the transport cross sections are decreasing. Resonancelike structures may occur especially for smaller wave numbers and higher densities due to the disappearance of bound states. Their contributions are taken over by the scattering states and the corresponding phase shifts accomplish jumps according to the Levinson theorem. However, this k region is not important for the calculation of the correlation functions d_{nm} (19).

IV. RESULTS FOR THE CONDUCTIVITY

The electrical conductivity has been determined via Eq. (17) inserting the density-dependent transport cross sections (28) and the respective composition of the plasma into the expressions for the correlations functions (24). These resulting conductivities are based on a realistic plasma composition within the present PIP model and account for the scattering processes of electrons at other electrons, all relevant ion species, and neutral atoms on T matrix level.

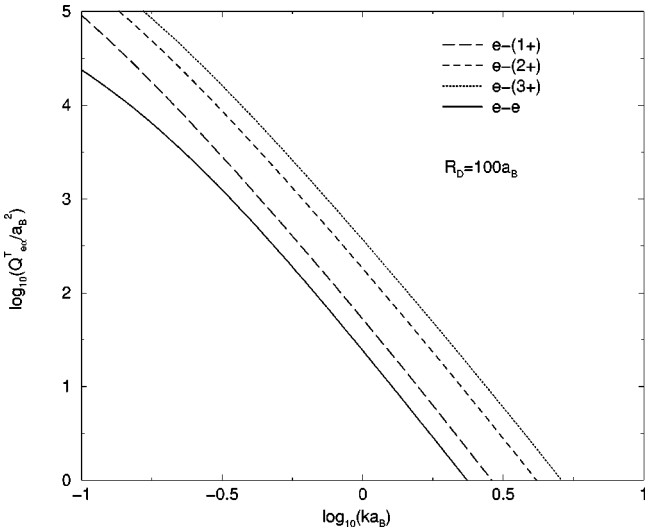

FIG. 5. Same as Fig. 3 but for a screening length of $R_D = 100a_B$.

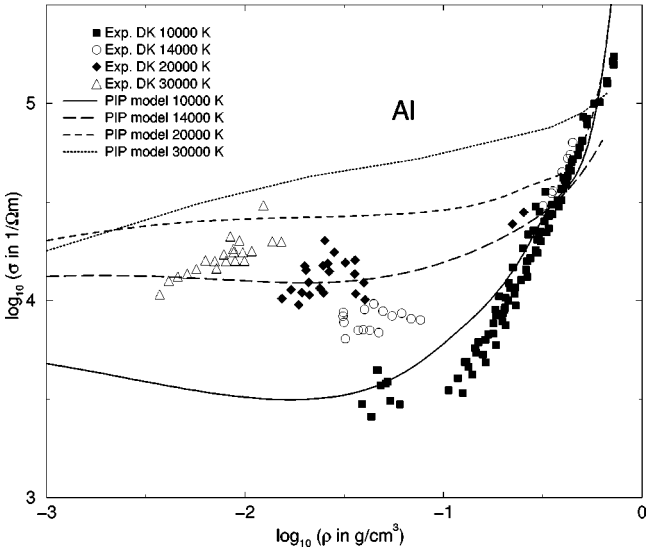

FIG. 6. Electrical conductivity of Al plasma for $T=(10–30)\times10^3$ K as a function of the density within the present PIP model (lines) compared with the experimental results of DeSilva and Katsouros (DK, data points) [10].

The conductivities are displayed in Figs. 6 and 7 for aluminum and copper plasma, respectively, as a function of the density for various temperatures. We compare first with results of DeSilva and Katsouros (DK) [10] for plasmas generated by rapid vaporization of metal wires in a water bath. These conductivities have been derived for densities from about 1/5 solid density down to 0.02 g/cm^3 and a temperature range of $(10–30)\times10^3$ K.

The theoretical conductivities approach the Spitzer values in the low-density limit. For higher densities and, especially, for low temperatures of $T\leqslant10^4$ K, the conductivities pass through a minimum around $\varrho\approx(0.05–0.1)$ g/cm^3. This special behavior is a result of the diminishing fraction of free electrons and their decreasing mobility due to scattering at neutral atoms. The experimental values of these minima are

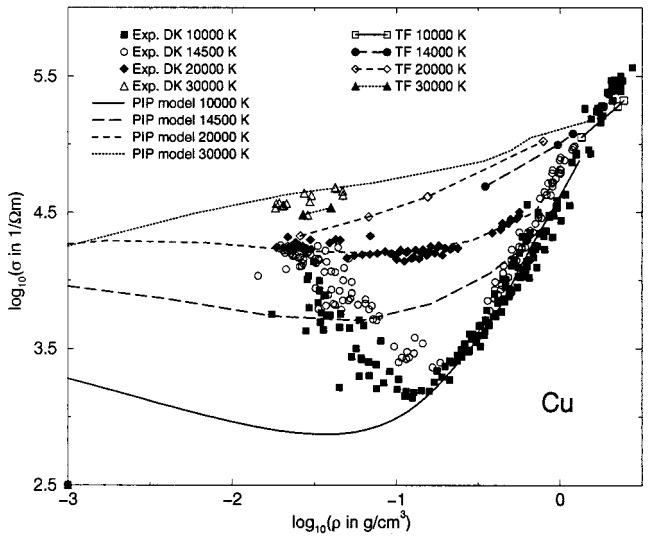

FIG. 7. Same as Fig. 6 but for Cu plasma. In addition, the conductivities of Tkachenko and Fernández de Córdoba (TF) [23] are shown (data points connected by lines).

much lower than the minimum metallic conductivity of $\sigma_{\min} \approx 2 \times 10^4\ \Omega^{-1}\mathrm{m}^{-1}$ as estimated by Mott for the solid at $T = 0$ K [48]. Then, the conductivities show a subsequent sharp increase which is a direct result of the increasing ionization degree due to the occurrence of the higher charged states, see Figs. 1 and 2. The behavior for the high-density domain above ϱ_0 can usually be described by the Ziman formula.

Using the Mott criterion for the minimum metallic conductivity in order to locate the corresponding nonmetal-to-metal transition also for finite temperatures, a critical density of about 0.3 g/cm^3 is found for Al and of 0.5 g/cm^3 for Cu, respectively. Below these densities, the expanded metal undergoes a transition to a partially ionized vapor with nonmetallic conductivity. This behavior is very similar to that found in static experiments for expanded metal fluids such as Cs [49] which has been explained theoretically also within the PIP model [22].

Although simple concepts have been applied for the plasma composition (coupled mass action laws) and the interactions between the charged particles (Debye potential), the overall agreement with the experimental conductivities of DeSilva and Katsouros [10] is good, especially for lower temperatures and the domain of higher densities where the strong increase of the conductivity occurs. The agreement with the Cu data is better than for Al and reasonable even for the higher temperatures. We conclude that the present PIP model is applicable for the description of expanded metal plasmas.

We show in Fig. 7 also the theoretical conductivities of Tkachenko and Fernández de Córdoba (TF) [23] which have been reported in Table III of their paper for copper plasma. Their alternative correlation function method is based on a generalized random phase approximation and applicable for fully ionized plasmas. The agreement with the experimental points of DeSilva and Katsouros is reasonable for conditions where the plasma is nearly fully ionized, i.e., for the higher temperatures and/or higher densities. For lower temperatures and not too high densities, greater discrepancies occur due to the neglect of partial ionization.

Systematic deviation between the experimental points and the present results within the PIP model have to be stated for the density region below 0.1 g/cm^3. The SESAME tables [50] have been used by DeSilva and Katsouros to analyze their experimental data, especially to determine the temperature. Furthermore, they have applied the Thomas-Fermi model of More [51] to calculate the ionization state Z_{eff}. However, both the SESAME tables and the Thomas-Fermi model become increasingly inaccurate when the plasma is no longer fully ionized. A chemical model as used here is more appropriate for the treatment of the partially ionized vapor where an electronic transition from metallic to nonmetallic conduction occurs.

Another series of experiments using the technique of rapid wire evaporation has been performed recently by Krisch and Kunze (KK) [12]. They vaporized Al wires in small glass capillaries by means of short pulse currents from an electrical discharge and produced nonideal plasmas with densities of (0.001–1.0) g/cm^3 and temperatures of $(7\text{–}24) \times 10^3$ K. Contrary to preceding measurements [9] and the data of DeSilva and Katsouros [10], they were able to determine the plasma parameters density *and* temperature spectroscopically so that no model for the equation of state has been used. We compare our results with their data and various theories for $T = 10\,000$ K and $T = 20\,000$ K in Figs. 8 and 9, respectively.

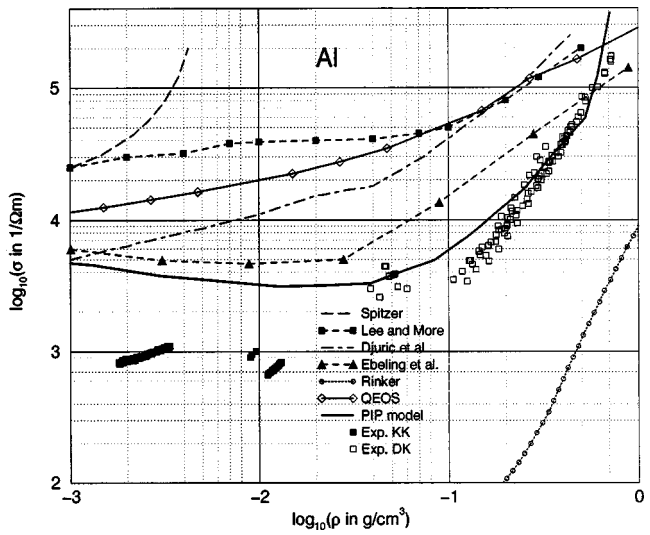

FIG. 8. Electrical conductivity of Al plasma for $T = 10\,000$ K as a function of the density within the present PIP model compared with the experimental results of Krisch and Kunze (KK) [12], those of DeSilva and Katsouros (DK) [10] from Fig. 6, and other theories (see text).

The new data of Krisch and Kunze continue the existing data points of DeSilva and Katsouros for 10 000 K and 20 000 K into the regions of lower and higher densities, respectively. In general, the results of the present PIP model approach the experimental points better than the other theories. However, the deviations still amount up to a factor of 2–4 for the region of low densities and temperatures. For higher densities above 0.1 g/cm^3, the agreement is much better.

The Spitzer theory is only applicable for the low-density region and fully ionized plasmas. The theory of Lee and More [43] is based on the relaxation time approximation for

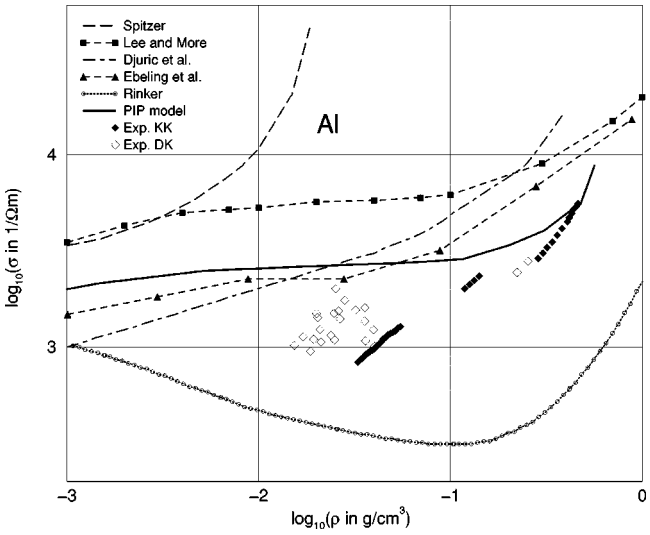

FIG. 9. Same as Fig. 8 but for $T = 20000$ K.

the solution of a Boltzmann transport equation valid for arbitrary degeneracy but neglects electron-electron scattering which yields an upper estimate for the plasma conductivity. The Rinker theory [17] is based on the Ziman formula. The ion-ion structure factor and the effective electron-ion potential are determined self-consistently. This treatment obviously gives a lower estimate for the plasma conductivity. The theories of of Ebeling *et al.* [30] and Djurić *et al.* [52] are derived for fully ionized plasmas and approach the experimental points much better than those of Lee and More and of Rinker. The consideration of neutral atoms in the present PIP model which are relevant especially for lower temperatures gives a further improvement.

In order to estimate the accuracy of equations of state based on the Thomas-Fermi theory in the expanded metal regime, we have taken into account the composition from the QEOS model [34] instead of the relative fractions as derived here for the case of Al plasma at 10 000 K, see Fig. 8. The respective conductivities converge to the experimental data around the solid state density ϱ_0, but are systematically higher up to one order of magnitude for lower densities.

With increasing density, further effects become of importance. For instance, the ion-ion structure factor has been included in the calculation of the electron-ion correlation function (26) on the level of the hypernetted chain approximation for high densities $\varrho=(0.1-1.0)\varrho_0$ as outlined in Ref. [21]. Only a small decrease of the conductivity of about 10% has been obtained for those conditions. Therefore structure factor effects as well as local-field corrections to the dielectric function become important for the conductivity only at still higher densities.

V. CONCLUSIONS

In this paper we have determined the electrical conductivity of dense aluminum and copper plasmas within a partially ionized plasma model, originally developed for hydrogen plasma [21]. We have considered a realistic plasma composition and the interactions of free electrons with other electrons, atoms, and the relevant ion species on T matrix level. The agreement with the available experimental data [10,12] is reasonable. In general, an improved understanding of the behavior of expanded metal plasmas can be gained within the present PIP model. Especially, the metal-to-nonmetal transition in the expanded, partially ionized vapor can be explained by the occurrence of neutral atoms. This has already been shown for expanded metal fluids such as Cs at lower temperatures [22]. The minimum behavior of the conductivity as found experimentally for low temperatures has been reproduced in the present study.

For a more sensitive treatment of the special metal properties compared with those of hydrogen [21], various improvements of the present approach are possible. For instance, the influence of non-Coulombic contributions to the electron-ion potentials has to be studied using self-consistent pseudopotentials rather than the Debye potential (29). Furthermore, higher charged states beyond $k=3$ may have an influence on the plasma properties at the highest densities considered here.

For the description of shock compressed matter, i.e., for $\varrho \geqslant \varrho_0$, the instability of the present equation of state has to be analyzed within a Maxwell construction which is the aim of future work. There, structure factor effects and dynamic screening including local-field corrections become of importance. This region of strongly coupled, fully ionized, multicomponent plasmas can be treated by self-consistent field theories as given, e.g., by Tkachenko and Fernández de Córdoba [23], The present approach can also be applied in that region considering the many-particle effects mentioned above.

The reason for the systematic discrepancies between the experimental conductivities and the present theoretical results at lower densities is probably the use of different equations of state. This has to be checked.

ACKNOWLEDGMENTS

I thank G. Röpke (Rostock), A. Förster (Berlin), and M. Schlanges (Greifswald) for helpful discussions. I am grateful to A. Wierling and R. Walke (Rostock) for technical assistance. I am indebted to A. W. DeSilva (College Park), H.-J. Kunze and I. Krisch (Bochum), and H. Hess and A. Kloss (Greifswald) for sending me their experimental data for the electrical conductivity. I thank A. Kemp (Garching) for making the results of the QEOS code available. This study was supported by the Deutsche Forschungsgemeinschaft within the Sonderforschungsbereich 198, *Kinetics of Partially Ionized Plasmas*.

[1] H. Minoo, C. Deutsch, and J.P. Hansen, Phys. Rev. A **14**, 840 (1976).
[2] E. Flowers and N. Itoh, Astrophys. J. **206**, 218 (1976).
[3] N. Itoh, S. Mitake, H. Iyetomi, and S. Ichimaru, Astrophys. J. **273**, 774 (1983).
[4] Yu.L. Ivanov, V.B. Mintsev, V.E. Fortov, and A.N. Dremin, Zh. Eksp. Teor. Fiz. **71**, 216 (1976) [Sov. Phys. JETP **44**, 112 (1976).
[5] R.L. Shepherd, D.R. Kania, and L.A. Jones, Phys. Rev. Lett. **61**, 1278 (1988).
[6] H.M. Milchberg, R.R. Freeman, S.C. Dacey, and R.M. More, Phys. Rev. Lett. **61**, 2364 (1988).
[7] G. Pottlacher, E. Kaschnitz, and H. Jäger, J. Non-Cryst. Solids **156–158**, 374 (1993).
[8] J.F. Benage, Jr., W.R. Shanahan, E.G. Sherwood, L.A. Jones, and R.J. Trainor, Phys. Rev. E **49**, 4391 (1994).
[9] A.W. DeSilva and H.-J. Kunze, Phys. Rev. E **49**, 4448 (1994).
[10] A.W. DeSilva and J.D. Katsouros, Phys. Rev. E **57**, 5945 (1998).
[11] A. Kloss, T. Motzke, R. Grossjohann, and H. Hess, Phys. Rev. E **54**, 5851 (1996).
[12] I. Krisch, Ph.D. thesis, Ruhr-Universität Bochum, 1997 (unpublished); I. Krisch and H.-J. Kunze, Phys. Rev. E **57**, 6557 (1998).
[13] J. Haun, I. Krisch, and H.-J. Kunze (unpublished).

[14] R. Redmer, Phys. Rep. **282**, 35 (1997).
[15] D.B. Boercker, F.J. Rogers, and H.E. DeWitt, Phys. Rev. A **25**, 1623 (1982); see also D. B. Boercker, *ibid.* **23**, 1969 (1981); F.J. Rogers, H.E. DeWitt, and D.B. Boercker, Phys. Lett. **82A**, 331 (1981).
[16] S. Ichimaru and S. Tanaka, Phys. Rev. A **32**, 1790 (1985).
[17] G.A. Rinker, Phys. Rev. B **31**, 4207 (1985); **31**, 4220 (1985); Phys. Rev. A **37**, 1284 (1988).
[18] D.N. Zubarev, *Nonequilibrium Statistical Thermodynamics* (Consultants Bureau, New York, 1974).
[19] G. Röpke, Physica A **121**, 92 (1983).
[20] G. Röpke, Phys. Rev. A **38**, 3001 (1988).
[21] H. Reinholz, R. Redmer, and S. Nagel, Phys. Rev. E **52**, 5368 (1995).
[22] R. Redmer, H. Reinholz, G. Röpke, R. Winter, F. Noll, and F. Hensel, J. Phys.: Condens. Matter **4**, 1659 (1992).
[23] I.M. Tkachenko and P. Fernández de Córdoba, Phys. Rev. E **57**, 2222 (1998).
[24] R. Zimmermann, *Many-Particle Theory of Highly Excited Semiconductors* (Teubner Verlagsgesellschaft, Leipzig, 1988), p. 150.
[25] W.D. Kraeft, D. Kremp, W. Ebeling, and G. Röpke, *Quantum Statistics of Charged Particle Systems* (Plenum, New York, 1986).
[26] S. Ichimaru, Rev. Mod. Phys. **54**, 1017 (1982). For a review of plasma parameters see also S. Ichimaru, *Plasma Physics* (Benjamin, Menlo Park, CA, 1986).
[27] W. Ebeling and W. Richert, Ann. Phys. (Leipzig) **39**, 362 (1982).
[28] W. Ebeling and W. Richert, Phys. Status Solidi B **128**, 467 (1985); Phys. Lett. **108A**, 80 (1985); Contrib. Plasma Phys. **25**, 1 (1985).
[29] A. Förster, Ph.D. thesis, Humboldt-Universität zu Berlin, 1991 (unpublished).
[30] W. Ebeling, A. Förster, V.E. Fortov, V.K. Gryaznov, and A.Ya. Polishchuk, *Thermophysical Properties of Hot Dense Plasmas* (Teubner Verlagsgesellschaft, Stuttgart, 1991), p. 39.
[31] R. Redmer, G. Röpke, and R. Zimmermann, J. Phys. B **20**, 4069 (1987).
[32] R. Redmer, T. Rother, K. Schmidt, W.D. Kraeft, and G. Röpke, Contrib. Plasma Phys. **28**, 41 (1988).
[33] M.H. Mittleman and K.M. Watson, Phys. Rev. **113**, 198 (1959).
[34] R. More, K. Warren, D. Young, and G. Zimmermann, Phys. Fluids **31**, 3059 (1988); see also A.J. Kemp, MPQ Report No. 229 (Garching), 1998 for the numerical code.
[35] L. Spitzer, Jr. and R. Härm, Phys. Rev. **89**, 977 (1953).
[36] J.M. Ziman, Philos. Mag. **6**, 1013 (1961).
[37] M. Baus, J.-P. Hansen, and L. Sjögren, Phys. Lett. **82A**, 180 (1981); H. Minoo, C. Deutsch, and J.-P. Hansen, Phys. Rev. A **14**, 840 (1976).
[38] H. Gould and H.E. DeWitt, Phys. Rev. **155**, 68 (1967); see also R.H. Williams and H.E. DeWitt, Phys. Fluids **12**, 2326 (1969).
[39] G. Röpke and R. Redmer, Phys. Rev. A **39**, 907 (1989).
[40] Yu.K. Kurilenkov and A.A. Valuev, Contrib. Plasma Phys. **24**, 529 (1984).
[41] R.J. Zollweg and R.W. Liebermann, J. Appl. Phys. **62**, 3621 (1987).
[42] R.B. Mohanti and J.G. Gilligan, J. Appl. Phys. **68**, 5044 (1990).
[43] Y.T. Lee and R.M. More, Phys. Fluids **27**, 1273 (1984).
[44] F.E. Höhne, R. Redmer, G. Röpke, and H. Wegener, Physica A **128**, 643 (1984).
[45] H. Reinholz, R. Redmer, and D. Tamme, Contrib. Plasma Phys. **29**, 395 (1989).
[46] F. Sigeneger, S. Arndt, R. Redmer, M. Luft, D. Tamme, W.D. Kraeft, G. Röpke, and T. Meyer, Physica A **152**, 365 (1988).
[47] S. Arndt, F. Sigeneger, F. Bialas, W.D. Kraeft, M. Luft, T. Meyer, R. Redmer, G. Röpke, and M. Schlanges, Contrib. Plasma Phys. **30**, 273 (1990).
[48] N.F. Mott, *Conduction in Non-Crystalline Materials* (Oxford University Press, Oxford, 1993), p. 26.
[49] F. Noll, W.-C. Pilgrim, and R. Winter, Z. Phys. Chem., Neue Folge **156**, 303 (1988).
[50] SESAME: The Los Alamos National Laboratory Equation of State Database, Report No. LA-UR-92-3407.
[51] R.M. More, in *Physics of Laser Plasmas*, edited by A.M. Rubenchik and S. Witkowski, Handbook of Plasma Physics Vol. 3 (Elsevier, Amsterdam, 1991), p. 70.
[52] Z. Djurić, A.A. Mihajlov, V.A. Nastasyuk, M.M. Popović, and L.M. Tkachenko, Phys. Lett. A **155**, 415 (1991). See also V.M. Adamyam, Z. Djurić, A.M. Ermolaev, A.A. Mihajlov, and I.M. Tkachenko, J. Phys. D **27**, 11 (1994); **27**, 927 (1994).